ChemComm

COMMUNICATION

View Article Online
View Journal | View Issue

Cite this: *Chem. Commun.*, 2020, **56**, 7613

Received 23rd April 2020,
Accepted 1st June 2020

DOI: 10.1039/d0cc02930k

rsc.li/chemcomm

Targeting specific cell organelles with different-faceted nanocrystals that are selectively recognized by organelle-targeting peptides†

Qilin Yu, [ab] Guizhu Wu,[a] Tong Zhang, [a] Xudong Zhao,[c] Zhen Zhou, [c] Lu Liu, *[a] Wei Chen *[a] and Pedro J. J. Alvarez *[d]

Targeting specific cellular organelles is an elusive therapeutic goal that could be achieved by manipulating nanocrystal facets. As proof of concept, different facet-engineered nanonods (high-energy (001) CdS and (001) CdSe, and low-energy (101) CdS and (110) CdSe) exploited selective binding by organelle-targeting peptides and subsequent intracellular protein sorting to inhibit specific organelles without significant cytotoxicity.

Organelle dysfunction is closely associated with commonly encountered diseases, such as immunodeficiency (endoplasmic reticulum (ER) dysfunction),[1,2] diabetes (mitochondrial dysfunction) and obesity (mitochondrial dysfunction).[3,4] Inhibiting specific organelles while maintaining the overall cell viability would enhance the treatment of such diseases.[5] One major challenge for achieving this elusive goal is the non-specific intracellular distribution of remedial agents,[6] which may result in unintended collateral damage to other cell constituents.

Sorting of natural proteins is a common process in mammalian cells that could be exploited to target specific cell organelles for inhibition or stimulation purposes.[7–12] We show proof-of-concept that the efficiency and selectivity of organelle-targeting and associated therapeutics could be significantly enhanced by using nanomaterials (NMs, CdS and CdSe nanorods) that are engineered to be recognized and preferentially bound by specific organelle-targeting peptides (OTPs) for subsequent delivery to the intended organelles (Scheme 1). Since exposed crystal facet is one of the most intrinsic NM surface properties controlling the reactivity, biorecognition, and intracellular uptake and toxicity of crystalline NMs,[13–16] it is plausible to achieve selective organelle-targeting through facet engineering.

We examined the biodistribution of four different-faceted Cd-based nanorods (high-energy (001) CdS and (001) CdSe, and low-energy (101) CdS and (110) CdSe) in two types of mammalian cells (*i.e.*, macrophages (NR8383) and normal fibroplasts (NIH3T3)) to assess response variability. All nanorods were synthesized with similar morphology, size and surface charge (Fig. 1 and Table S1, ESI†) to discern the effects of exposed facets, which have been overlooked in the context of intracellular NM delivery. We report facet-dependent nanorods biodistribution in viable cells, with subsequent organelle-specific inhibition. Low-energy-faceted nanorods were preferentially bound to the mitochondria and caused more damage to this organelle despite similar cellular uptake as high-energy-faceted nanorods. In contrast, high-energy-faceted nanorods accumulated preferentially in the ER and the adjacent (interconnected) nucleus. This biodistribution pattern is attributed to the demonstrated preferential binding of nanorods with different crystal facets by specific OTPs, which suggests that intracellular

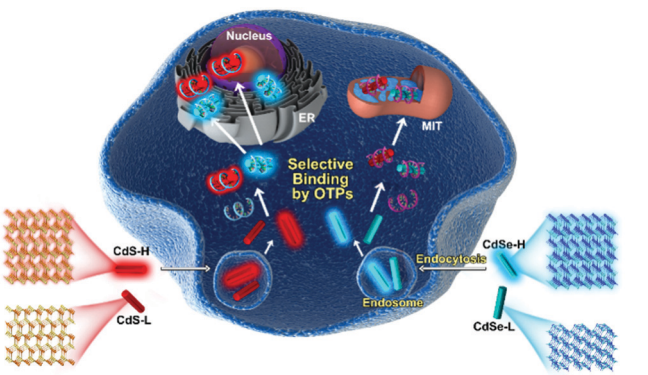

Scheme 1 Schematic illustration of facet-engineered nanorods for targeting of specific organelles. The blue and red spiral lines indicate the ER-targeting peptide and the mitochondrion-targeting peptide, respectively.

[a] *College of Environmental Science & Eng., Nankai University, Tianjin 300350, China. E-mail: liul@nankai.edu.cn, chenwei@nankai.edu.cn*
[b] *Key Laboratory of Molecular Microbiology & Technology, College of Life Sciences, Nankai University, Tianjin 300071, China*
[c] *College of Materials Science & Eng., Nankai University, Tianjin 300350, China*
[d] *Department of Civil & Environ. Eng., Rice University, Houston, TX, 77005, USA. E-mail: alvarez@rice.edu*

† Electronic supplementary information (ESI) available. See DOI: 10.1039/d0cc02930k

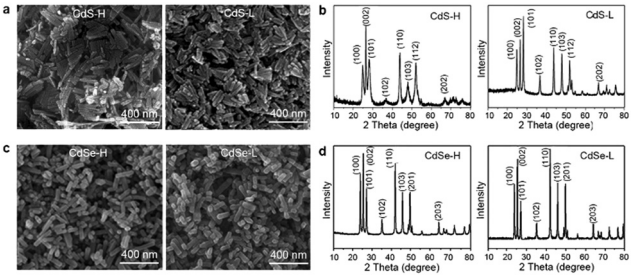

Fig. 1 Scanning electron microscopy (SEM) images (a and c) and X-ray diffraction (XRD) patterns (b and d) of CdS-H, CdS-L, CdSe-H and CdSe-L. The suffixes "H" and "L" represent high-energy-faceted and low-energy-faceted nanorods, respectively.

protein sorting could be exploited through nanocrystal facet engineering for precise subcellular delivery of NMs.

We examined the intracellular distribution of different nanorods in rat macrophages NR8383 after co-incubating the nanorods and cells for 48 h in culture medium. For both CdS and CdSe, cellular uptake was statistically undistinguishable ($p > 0.05$) for the corresponding high-energy-faceted nanorods (referred to as "CdS-H" and "CdSe-H" hereafter) and low-energy-faceted nanorods ("CdS-L" and "CdSe-L") (Fig. S1, ESI†). However, both CdS and CdSe showed facet-dependent preferential (but not exclusive) binding to different organelles (Fig. 2 and Fig. S2, S3, ESI†). Regardless of elemental composition, high-energy-faceted nanorods were preferably associated with the ER and the nucleus. For example, for the CdS-H-treated cells, 24% of the ER harbored nanorods, whereas for the CdS-L-treated cells, nanorods were associated with only 6% of the observed ER; similarly, CdS-H was associated with 10% of the observed nuclei, compared to 2% for CdS-L (Fig. 2a and b). In contrast, low-energy-faceted nanorods were preferentially associated with mitochondria. Specifically, 35% of mitochondria in the cells exposed to CdS-L accumulated these nanorods, whereas merely 3% of mitochondria accumulated CdS-H (Fig. 2a and b). Similar trends were observed for CdSe nanorods (Fig. 2c and d).

During mammalian cellular uptake, NMs are known to contact and become enveloped by the plasma membrane, and form NM-contained endosomes.[17–20] Endocytosed NMs are transported into the lysosomes, and are widely reported to subsequently escape from the endosomes or lysosomes to the cytoplasm by disruption of the endosome/lysosome membrane,[21] thus becoming available for capping by intracellular proteins.[22–24] ICP analysis showed little dissolution of nanorods (*i.e.*, low levels of released Cd^{2+}) in acidic solutions (<0.08 mg L^{-1}, pH = 5.5) and in cells (<0.12 mg L^{-1}) (Fig. S4, ESI†), indicating stability in the endosomes/lysosomes before and after escaping. Accordingly, further NM transport to different organelles could be mediated by specific OTPs (as the components of protein corona) found in the cytoplasm. The transport and distribution of such OTPs are determined by specific signal peptide sequences that are part of the proteins' primary structure.[25] Thus, we postulate that the differential organelle distribution of high- *versus* low-energy nanorods is due to their different affinities to mitochondrion-targeting *versus* ER-targeting peptides.

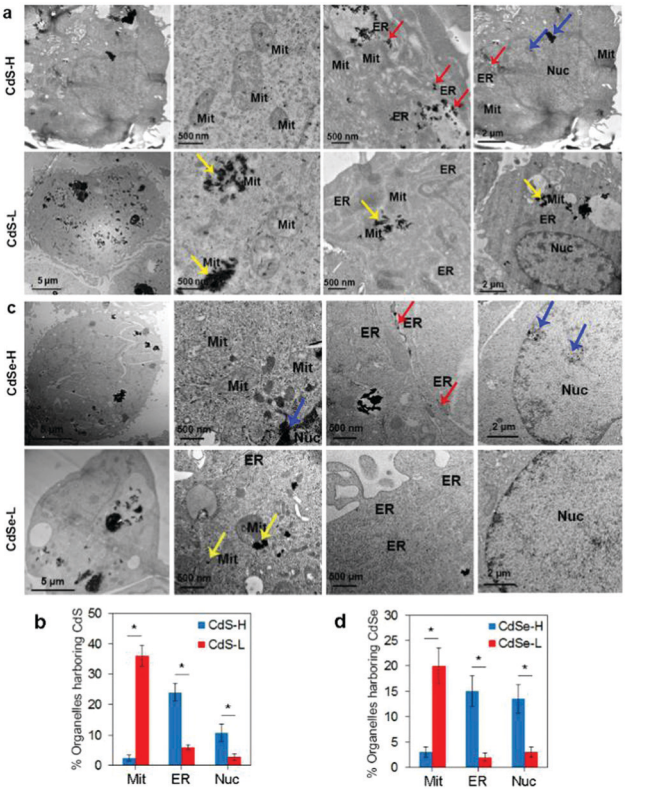

Fig. 2 CdS(e)-H and CdS(e)-L exhibit preferential accumulation in different organelles in NR8383 cells. Transmission electron microscopy images show that CdS-H and CdSe-H (20 mg L^{-1}, 48 h exposure) preferentially accumulated in the endoplasmic reticulum (ER) and interconnected nucleus (Nuc), whereas CdS-L and CdSe-L primarily accumulated in the mitochondria (Mit) (a and c). The yellow, red and blue arrows show CdS/CdSe nanorods accumulated in the mitochondria, ER and nuclei, respectively. The mitochondria, ER or nucleus harboring CdS/CdSe were further quantified (b and d). At least 100 mitochondria, ER or nucleus were counted, and the number of organelles harboring nanorods was normalized to the total number of quantified organelles. Asterisks (*) indicate significant difference between CdS(e)-H and CdS(e)-L ($p < 0.05$) ($n = 3$).

To test this hypothesis, we measured the affinity of high-energy and low-energy-faceted nanorods to mitochondrion- and ER-targeting consensus peptide sequences (*i.e.*, Cha-D-Arg-Cha-Lys-Cha-D-Arg-Cha-Lys, Met-Lys-Trp-Val-Thr-Phe-Ile-Ser-Leu-Leu-Phe-Leu-Phe-Ser-Ser-Ala-Tyr-Ser, respectively).[26–31] Consistent with our hypothesis, the ER-targeting peptide exhibited stronger adsorption affinity for high-energy-faceted than for low-energy-faceted nanorods, while the opposite trend was observed for the mitochondrion-targeting peptide (Fig. 3). The significantly higher affinity of the mitochondrion-targeting peptide for CdS-L (275% higher than for CdS-H, Fig. 3a) or CdSe-L (35% higher than for CdSe-H, Fig. 3b) is noteworthy because low-energy-faceted nanocrystals were less reactive than high-energy-faceted nanocrystals in BSA protein adsorption tests.[13] Moreover, an actin cytoskeleton-targeted peptide (Met-Gly-Val-Ala-Asp-Leu-Ile-Lys-Lys-Phe-Glu-Ser-Ile-Ser-Lys-Glu-Glu),[32–34] which was used as negative control, exhibited similarly low adsorption affinity for both high- and low-energy-faceted nanorods (Fig. 3). These results indicate that facet-dependent binding of nanorods

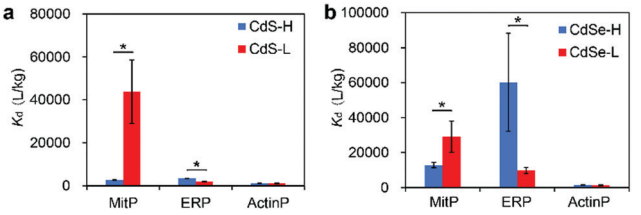

Fig. 3 Mitochondria-targeting peptides (MitP) preferentially bind to low-energy-faceted nanorods (L), whereas ER-targeting peptides (ERP) have higher affinity for high-energy-faceted nanorods (H), and actin-targeting peptides (ActinP, negative control) have similarly low affinity for both CdS (a, 100 mg L^{-1}) and CdSe (b, 100 mg L^{-1}). K_d is the distribution coefficient of peptides between adsorbed and solution phases (L kg^{-1}), calculated as $(C_0 - C_e)/(C_{nanorod} \cdot C_e)$, where C_0 is the initial peptide concentration in solution, C_e is its equilibrium concentration in solution, and $C_{nanorod}$ is the CdS or CdSe concentration in solution. Asterisks (*) indicate significant difference between the corresponding high- and low-energy nanorods ($p < 0.05$) ($n = 3$).

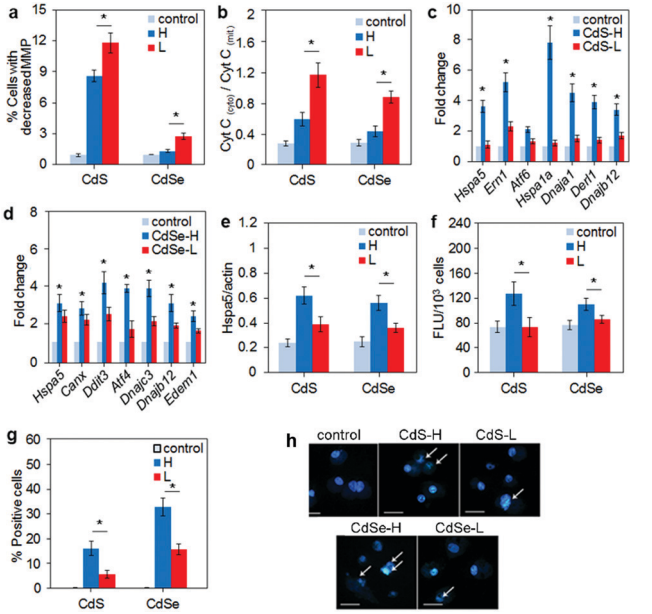

Fig. 4 Low-energy (L) nanorods cause more severe mitochondrial damage than high-energy (H) nanorods (a and b), while high-energy (H) nanorods cause more severe damage to ER (c–f) and nucleus (g and h) than low-energy (L) nanorods, for both CdS and CdSe (20 mg L^{-1}, 48 h exposure) in NR8383 cells. (a) MMP assay for the CdS-/CdSe-treated cells. (b) Cytochrome *C* (Cyt *C*) released from the mitochondria (Cyt $C_{(mit)}$) to cytoplasm (Cyt $C_{(cyto)}$). (c and d) qRT-PCR analyses of UPR genes. (e) Western blotting of Hspa5. (f) Ca^{2+} levels. (g) Comet assays. (h) DAPI staining. The white arrows in (h) indicate damaged nuclei. Scale bar = 20 μm. Asterisks (*) indicate significant difference between the nanorods ($p < 0.05$) ($n = 3$).

by different organelle-targeting peptides contributed to the organelle-specific association.

Preferential association of low-energy-faceted nanorods with mitochondria resulted in selective damage to the organelles. For example, MitoTracker staining showed that the cells treated with CdS-H (or CdSe-H) had healthy network-like mitochondria, whereas cells treated with CdS-L (or CdSe-L) exhibited dotted mitochondria, indicative of damage (Fig. S5, ESI†). Mitochondrial membrane potential (MMP) measurements and Cyt *C* blotting corroborated that CdS-H (or CdSe-H) caused less decrease of MMP (Fig. 4a) and lower levels of Cyt *C* released from the mitochondria to the cytoplasm than CdS-L (or CdSe-L) (Fig. 4b). Similar results were observed with NIH3T3 cells (Fig. S6, ESI†), encouraging further studies to determine whether facet engineering of nanocrystals could be used to selectively inhibit mitochondria to treat diseases such as diabetes and hypertriglyceridemia.[35,36]

Similarly, preferential association of high-energy-faceted nanorods with ER and nuclei resulted in selective damages to these organelles. ER dysfunction may induce activation of the unfolded protein response (UPR) pathway, resulting in up-regulation of UPR genes to alleviate this stress.[37–39] Moreover, ER stress may activate plasma membrane calcium channels, resulting in extracellular calcium influx and consequent elevation of intracellular Ca^{2+} levels.[40] Thus, we assessed ER dysfunction by quantifying upregulation of UPR genes and intracellular Ca^{2+} levels. Quantitative reverse transcription polymerase chain reaction (qRT-PCR) and transcription profiling analysis revealed that treatment with high-energy-nanorods induced higher expression of UPR genes (*e.g.*, *Hspa5*, *Ern1*, *Atf6* and *Dnajb12*) than treatment with low-energy nanorods (Fig. 4c, d and Fig. S7, ESI†). These expression data were confirmed by Western blotting for the UPR-related protein Hspa5. The Hspa5 levels were significantly higher in high-energy-nanorod-treated cells (Fig. 4e). Also, CdS-H caused a remarkable increase of intracellular Ca^{2+} levels in tested cells (Fig. 4f and Fig. S8, ESI†). Similar results were observed for CdSe nanorods, where the high-energy-nanorods preferentially damaged the ER (Fig. 4d–f and Fig. S8, ESI†).

The ER is closely associated with the nucleus (they are both part of the endomembrane system),[41] which was also more susceptible to damage by high-energy-faceted nanorods. For example, comet assays showed that CdS-H damaged a greater percentage of observed nuclei (15%) than CdS-L (6%) (Fig. 4g). 4′,6-Diamidino-2-phenylindole (DAPI) staining also showed that CdS-H caused more severe nuclear fragmentation than CdS-L (Fig. 4h). Moreover, higher levels of both HDAC1 and TyrRs, whose up-regulation indicates nucleus damage, were observed in the CdS-H-treated than in the CdS-L-treated cells (Fig. S8, ESI†). Similar results were observed for CdSe nanorods, where the high-energy nanorods preferentially damaged the nucleus (Fig. 4g, h and Fig. S9, ESI†). Overall, high-energy-faceted nanorods exerted greater damage to the ER and the nucleus and less damage to the mitochondria, while the opposite trend was observed for low-energy-faceted nanorods.

Recent research advances in medical practice indicate that an effective approach for treating certain diseases such as immunodeficiency, diabetes and obesity is inhibiting organelle functions without significantly hindering cell viability.[1,2] An interesting observation is that cells treated with Cd-based nanorods exhibited high viability (assessed per succinate dehydrogenase activity, Fig. S10, ESI†) while experiencing organelle damage (Fig. 4). For example, 91% of the cells remained viable and only 8% of the cells appeared apoptotic after 48 h treatment with CdS-H (Fig. S9, ESI†), even though both ER and

nucleus were damaged in those cells (Fig. 4c–h). Similarly, up to 92% of the cells remained viable and only 5.4% were apoptotic after treatment with CdSe-L (Fig. S10, ESI†), while the extent of mitochondrial damage was significant with this treatment (Fig. 4a and b). Similar results were observed with NIH3T3 cells (Fig. S11, ESI†). Thus, targeting organelles (and resulting damage) might be achieved while minimizing cell mortality, a trait that is critical for treating certain diseases.[42] For example, to treat immunodeficiency, it is desirable to activate the UPR pathway without killing the immune cells.[1,2] To treat diabetes, it is desirable to suppress mitochondrial activity without killing the normal cells.[3,4]

Another important implication of these results is that cell mortality could be mitigated by carefully choosing both the facet structure and the elemental composition of nanocrystals. For example, for high-energy (H) nanorods, CdS treatment resulted in higher cell viability, lower apoptosis and lower necrosis relative to the CdSe treatment (Fig. S10 and S11, ESI†), which renders CdS-H a better candidate for targeting ER and nucleus. In contrast, for low-energy (L) nanorods, CdSe resulted in less cell mortality than CdS (Fig. S10 and S11, ESI†), and therefore CdSe-L could be more advantageous in the application of NMs for targeting mitochondria without significantly compromising cell viability. The opposite tendency between CdS and CdSe with high- and low-energy facets likely reflects different elemental compositions (S or Se) exerting different biological effects. This implies that nanocrystals with specific organelle-targeting capabilities (through exposed crystal facet manipulation) and modulated toxicity (through elemental composition) could be designed for biomedical applications.

Overall, this study uncovers an overlooked link between exposed nanocrystal facets and organelle-specific interactions *via* specific organelle targeting peptides. Our results point to the great potential of nanocrystal facet engineering combined with protein sorting for efficient and precise subcellular delivery of NMs. This discovery not only enhances the possibility of selective organelle inhibition while minimizing cell mortality, which is highly desirable for the treatment of several organelle dysfunction-related diseases, but also has important implications for designing accurate and robust sub-cellular drug delivery systems. As caveat, we recognize that Cd-based nanomaterials may not be appropriate for many *in vivo* biomedical applications due to their potential toxicity. However, these results offer proof-of-concept that specific organelle targeting can be achieved by facet engineering of inorganic nanomaterials.

We acknowledge the support of National Natural Science Foundation of China (Grants 21425729, 31870139, and 21271108), and the NEWT ERC (NSF grant EEC-1449500).

Conflicts of interest

There are no conflicts to declare.

Notes and references

1 I. Kim, W. Xu and J. C. Reed, *Nat. Rev. Drug Discovery*, 2008, **7**, 1013.
2 V. Bigley, U. Cytlak and M. Collin, *Semin. Cell Dev. Biol.*, 2019, **86**, 50.
3 B. B. Lowell and G. I. Shulman, *Science*, 2005, **307**, 384.
4 W. Song, E. Owusu-Ansah, Y. Hu, D. Cheng, X. Ni, J. Zirin and N. Perrimon, *Proc. Natl. Acad. Sci. U. S. A.*, 2017, **114**, 8596.
5 N. M. Sakhrani and H. Padh, *Drug Des., Dev. Ther.*, 2013, **7**, 585.
6 L. Rajendran, H. J. Knölker and K. Simons, *Nat. Rev. Drug Discovery*, 2010, **9**, 29.
7 H. Lomas, I. Canton, S. MacNeil, J. Du, S. P. Armes, A. J. Ryan and G. Battaglia, *Adv. Mater.*, 2007, **19**, 4238.
8 A. M. Derfus, W. C. Chan and S. N. Bhatia, *Adv. Mater.*, 2004, **16**, 961.
9 X. H. Wang, H. S. Peng, L. Yang, F. T. You, F. Teng, L. L. Hou and O. S. Wolfbeis, *Angew. Chem., Int. Ed.*, 2014, **126**, 12679.
10 A. Jhaveri and V. Torchilin, *Expert Opin. Drug Delivery*, 2016, **13**, 49.
11 S. G. Garg and S. B. Gould, *Trends Cell Biol.*, 2016, **26**, 894.
12 E. A. Costa, K. Subramanian, J. Nunnari and J. S. Weissman, *Science*, 2018, **359**, 689.
13 L. Liu, M. Sun, H. Zhang, Q. Yu, M. Li, Y. Qi, C. Zhang, G. Gao, Y. Yuan and H. Zhai, *et al.*, *Nano Lett.*, 2015, **16**, 688.
14 F. Wu, W. Chen, B. Gillis, C. Fischbach, L. A. Estroff and D. Gourdon, *Biomaterials*, 2017, **116**, 174.
15 S. K. Ramakrishnan, M. Martin, T. Cloitre, L. Firlej and C. Gergely, *Phys. Chem. Chem. Phys.*, 2015, **17**, 4193.
16 L. Ruan, H. Ramezani-Dakhel, C. Y. Chiu, E. Zhu, Y. Li, H. Heinz and Y. Huang, *Nano Lett.*, 2013, **13**, 840.
17 D. Lison and F. Huaux, *Nat. Nanotechnol.*, 2011, **6**, 332.
18 S. Zhang, J. Li, G. Lykotrafitis, G. Bao and S. Suresh, *Adv. Mater.*, 2009, **21**, 419.
19 M. Li, M. Ehlers, S. Schlesiger, E. Zellermann, S. K. Knauer and C. Schmuck, *Angew. Chem., Int. Ed.*, 2016, **55**, 598.
20 J. L. West and N. J. Halas, *Annu. Rev. Biomed. Eng.*, 2003, **5**, 285.
21 J. Chen, J. Li, J. Zhou, Z. Lin, F. Cavalieri, E. Czuba-Wojnilowicz, Y. Hu, A. Glab, Y. Ju, J. J. Richardson and F. Caruso, *ACS Nano*, 2019, **13**, 11653.
22 M. Li, M. Ehlers, S. Schlesiger, E. Zellermann, S. K. Knauer and C. Schmuck, *Angew. Chem., Int. Ed.*, 2016, **55**, 598.
23 E. González-Domínguez, E. González-Lavado, L. Marín-Caba, B. Vaz, M. Pérez-Lorenzo, M. A. Correa-Duarte and M. L. Fanarraga, *Angew. Chem., Int. Ed.*, 2017, **56**, 13736.
24 T. Xia, M. Kovochich, M. Liong, H. Meng, S. Kabehie, J. I. Zink and A. E. Nel, *ACS Nano*, 2009, **3**, 3273.
25 G. von Heijne, *J. Membr. Biol.*, 1990, **115**, 195.
26 K. L. Horton, K. M. Stewart, S. B. Fonseca, Q. Guo and S. O. Kelley, *Chem. Biol.*, 2008, **15**, 375.
27 Q. Yu, Y. M. Zhang, Y. H. Liu, X. Xu and Y. Liu, *Sci. Adv.*, 2018, **4**, eaat2297.
28 B. Zhang, Q. Yu, Y. M. Zhang and Y. Liu, *Chem. Commun.*, 2019, **55**, 12200.
29 B. Martoglio and B. Dobberstein, *Trends Cell Biol.*, 1998, **8**, 410.
30 R. J. Perry, T. Kim, X. M. Zhang, H. Y. Lee, D. Pesta, V. B. Popov, D. Zhang, Y. Rahimi, M. J. Jurczak and G. W. Cline, *et al.*, *Cell Metab.*, 2013, **18**, 740.
31 T. Omura, *J. Biochem.*, 1998, **123**, 1010.
32 J. Riedl, A. H. Crevenna, K. Kessenbrock, J. H. Yu, D. Neukirchen, M. Bista and M. Sixt, *Nat. Methods*, 2008, **5**, 605.
33 Q. Yu, B. Zhang, J. Li and M. Li, *Chem. Commun.*, 2017, **53**, 11433.
34 Q. Yu, B. Zhang, Y. M. Zhang, Y. H. Liu and Y. Liu, *ACS Appl. Mater. Interfaces*, 2020, **12**, 13709.
35 J. A. Harper, K. Dickinson and M. D. Brand, *Obes. Rev.*, 2001, **2**, 255.
36 C. Hetz, *Nat. Rev. Mol. Cell Biol.*, 2013, **14**, 404.
37 R. Chen, L. Huo, X. Shi, R. Bai, Z. Zhang, Y. Zhao, Y. Chang and C. Chen, *ACS Nano*, 2014, **8**, 2562.
38 I. Tabas and D. Ron, *Nat. Cell Biol.*, 2011, **13**, 184.
39 C. Hetz and F. R. Papa, *J. Mol. Cell Biol.*, 2018, **69**, 169.
40 K. Mochida, Y. Oikawa, Y. Kimura, H. Kirisako, H. Hirano, Y. Ohsumi and H. Nakatogawa, *Nature*, 2015, **522**, 359.
41 G. S. Hotamisligil, *Nature*, 2006, **444**, 860.
42 S. Feske, Y. Gwack, M. Prakriya, S. Srikanth, S. H. Puppel, B. Tanasa, G. Patrick, P. G. Hogan, R. S. Lewis and M. Daly, *et al.*, *Nature*, 2006, **441**, 179.

